Varied forms of lamellar $[Sn_3Se_7]_n^{2n-}$ anion: the competitive and synergistic structural directing effects of metal-amine complex and imidazolium cations

Cheng–Feng Du,[a,b] Jian–Rong Li,*[a] Mei–Ling Feng,[a] Guo-Dong Zou,[c] Nan–Nan Shen[a,b] and Xiao–Ying Huang[a]

[a] State Key Laboratory of Structural Chemistry, Fujian Institute of Research on the Structure of Matter, Chinese Academy of Sciences, Fuzhou, Fujian 350002, P. R. China. Fax: (+86) 591-63173145

[b] University of Chinese Academy of Sciences, Beijing, 100049, People's Republic of China.

[c] College of Chemistry and Chemical Engineering, Xinyang Normal University, Xinyang 464000, China

E-mail: jrli@fjirsm.ac.cn

Supporting Information

1. Structure details

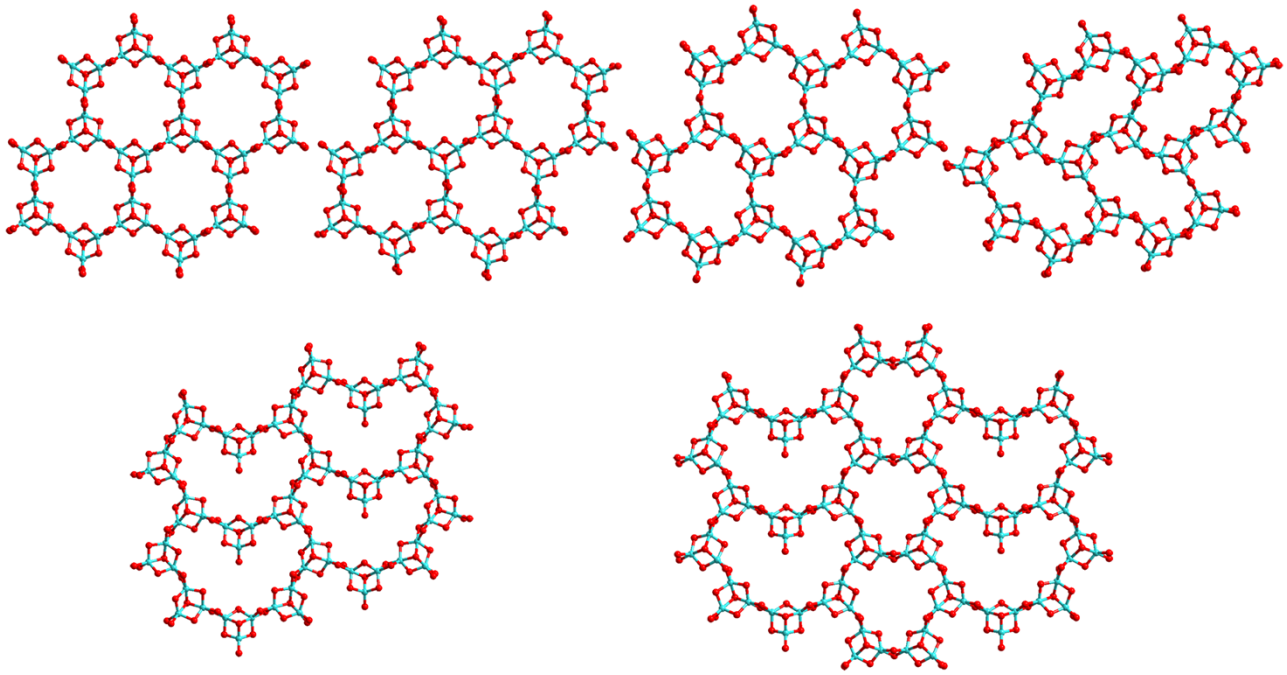

Figure S1. The four known lamellar $[Sn_3Se_7]_n^{2n-}$ anions with six–membered rings (up) and two novel lamellar $[Sn_3Se_7]_n^{2n-}$ anions with eight-membered heart-shaped rings (down) reported in this work.

When $[Sn_3Se_4]$ semi-cube was used as a node and $(\mu_2–Se)_2$ as a ligand, the lamellar $[Sn_3Se_7]_n^{2n-}$ anions in compounds **1**, **2**, **3** and **4** can be simplified as those in Figs. S2-S4, that is, compounds **1** and **2** contains a simplified elliptic six-membered ring while a novel eight-membered heart shaped ring can be found in **3** and **4**.

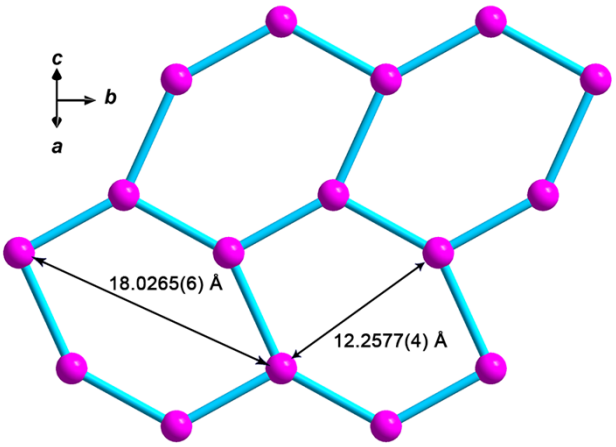

Figure S2. The simplified elliptic six-membered ring with $[Sn_3Se_4]$ semi-cube as a node and $(\mu_2–Se)_2$ as a ligand in **1** and **2**.

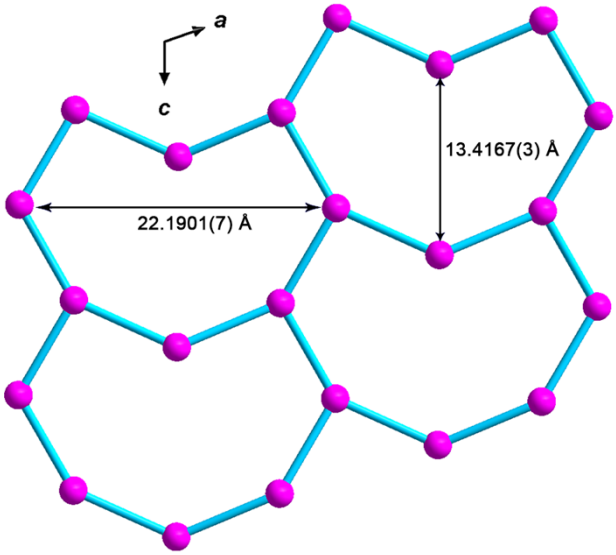

Figure S3. The simplified eight-membered heart shaped ring with $[Sn_3Se_4]$ semi-cube as a node and $(\mu_2–Se)_2$ as a ligand in **3**.

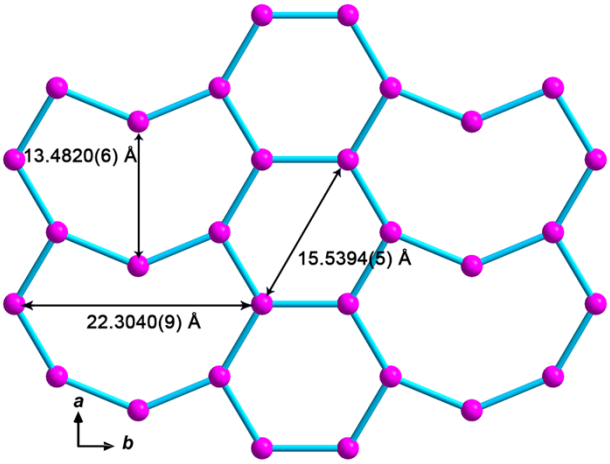

Figure S4. The simplified eight-membered heart shaped ring and six-membered ring with $[Sn_3Se_4]$ semi-cube as a node and $(\mu_2–Se)_2$ as a ligand in **4**.

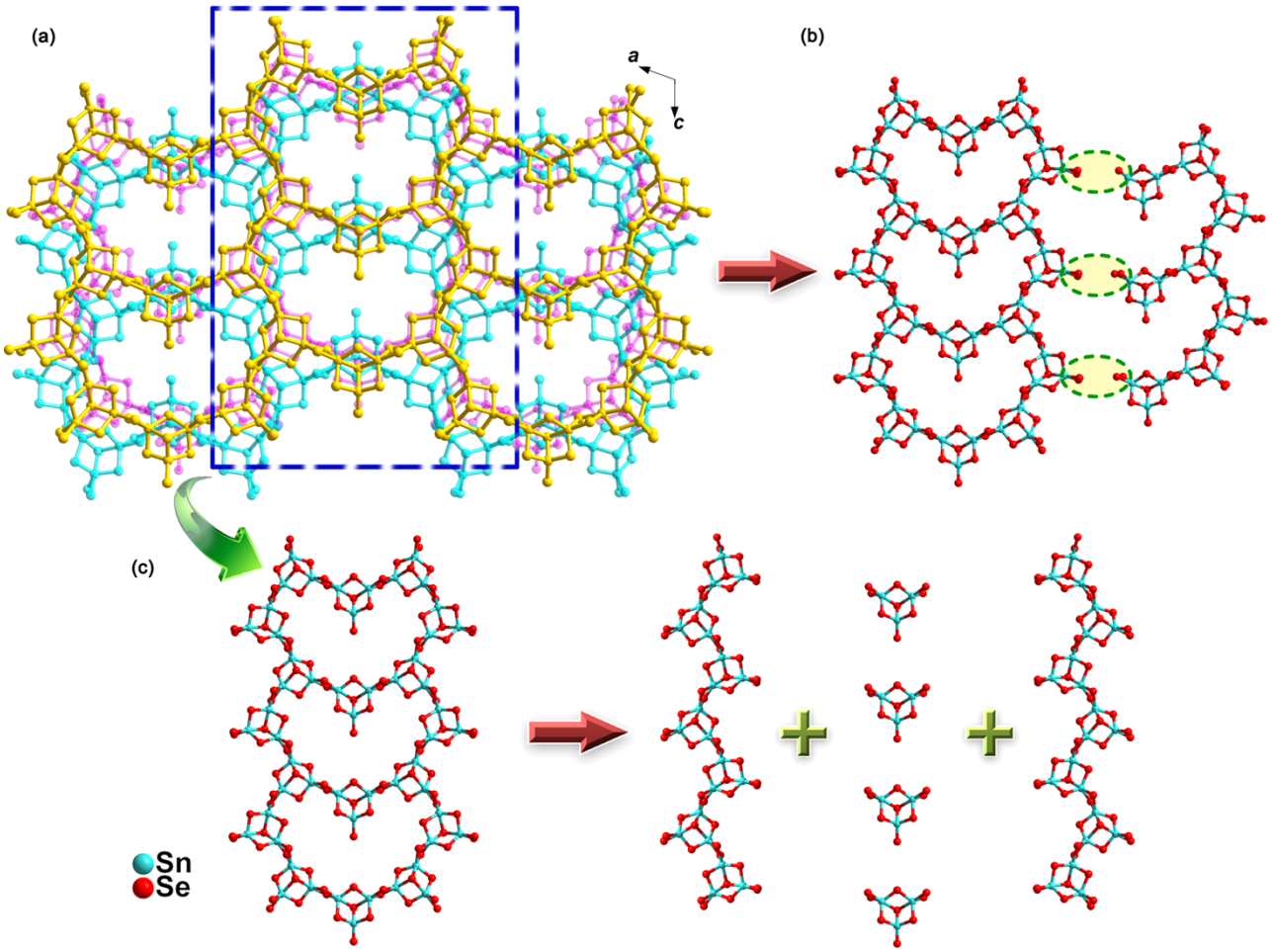

Figure S5. (a) A view of the packing of $[Sn_3Se_7]_n^{2n-}$ layers in **3** along the *b* axis, (b) the connecting mode of eight-membered heart shaped ring chain in **3** and (c) the eight-membered heart shaped ring chain constructed from the $[Sn_3Se_7]_n^{2n-}$ single chain and $[Sn_3Se_9]$ SBUs.

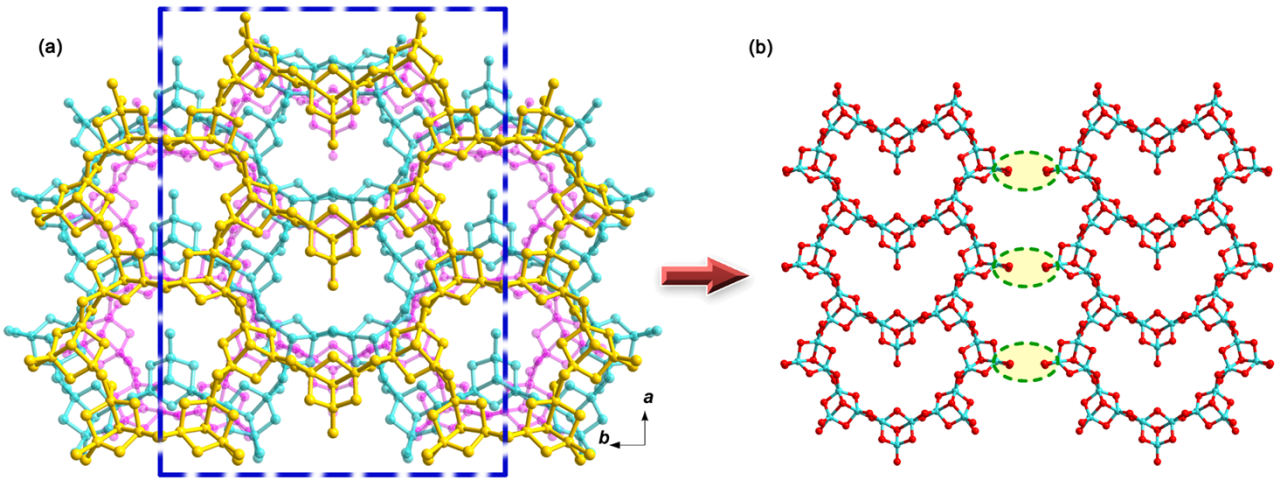

Figure S6. (a) A view of the packing of $[Sn_3Se_7]_n^{2n-}$ layers in **4** along the *c* axis and (b) the construction of eight-membered heart shaped ring chain in **4**.

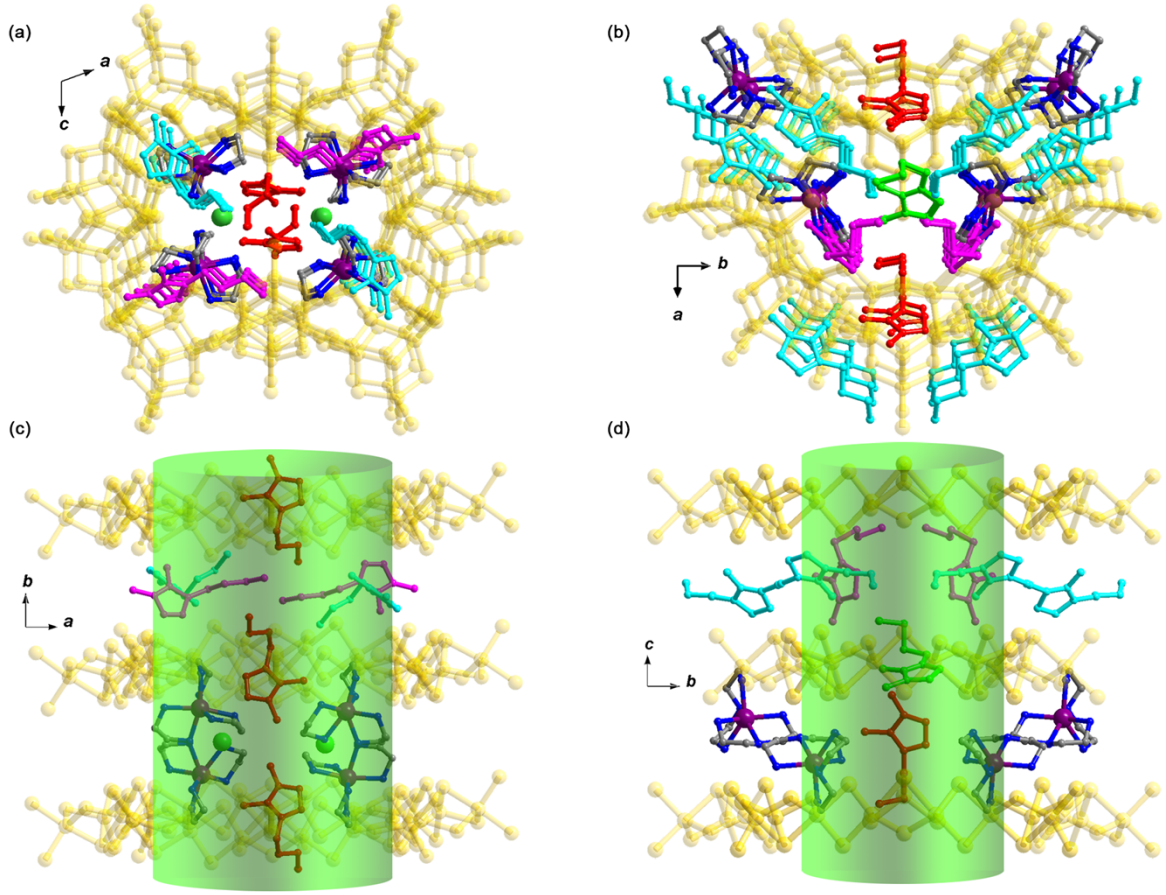

Figure S7. Perspective views of the mixed cations filling modes in compounds **3** (a) and **4** (b); the $[Sn_3Se_7]_n^{2n-}$ layers are in a yellow ball-stick mode, and the $[Bmmim]^+$ cations in different positions are distinguished by different colors. (c) and (d) show the side views of the mixed cations located in the inter-lamellar space and voids; the green cylinders indicate the channels in **3** and **4**.

2. Physical measurements

3a). PXRD

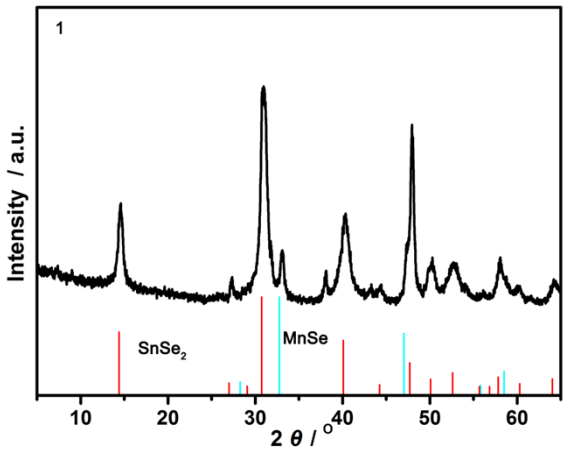

Figure S8. The PXRD pattern of the post-TGA residue of compound **1** along with the simulated ones of $SnSe_2$ and MnSe at bottom for comparison. The TGA residue of compound **1** is identified as a mixture of $SnSe_2$ and MnSe.

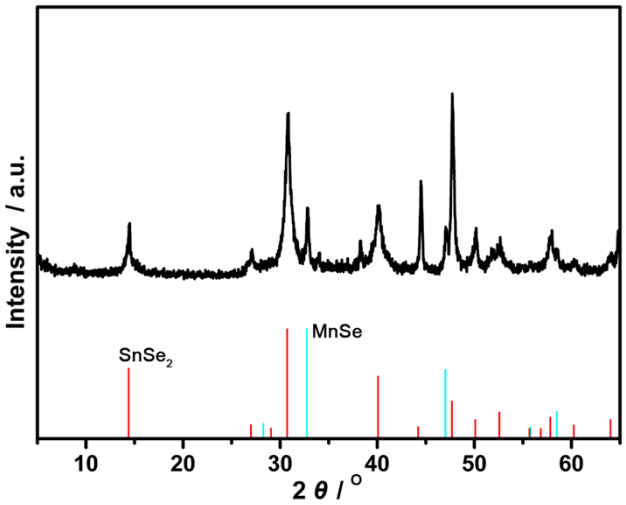

Figure S9. The PXRD pattern for the post-TGA residues of compound **2** along with the simulated ones of $SnSe_2$ and MnSe at bottom for comparison. The residue of compound **2** is identified as a mixture of $SnSe_2$ and MnSe.

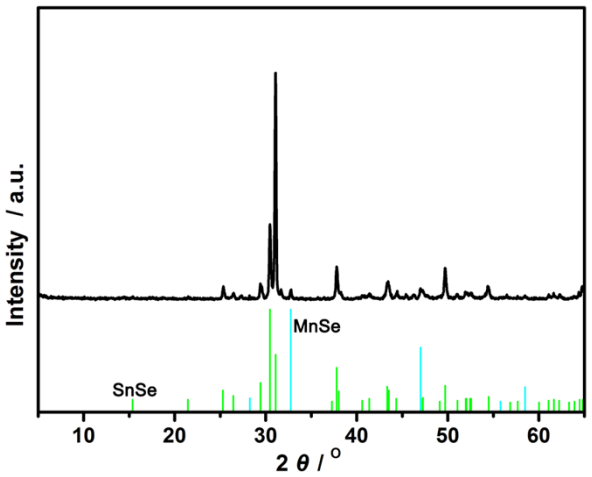

Figure S10. The PXRD pattern for the post-TGA residue of compound **3** along with the simulated ones of SnSe and MnSe at bottom for comparison. The residue of compound **3** is identified as a mixture of SnSe and MnSe.

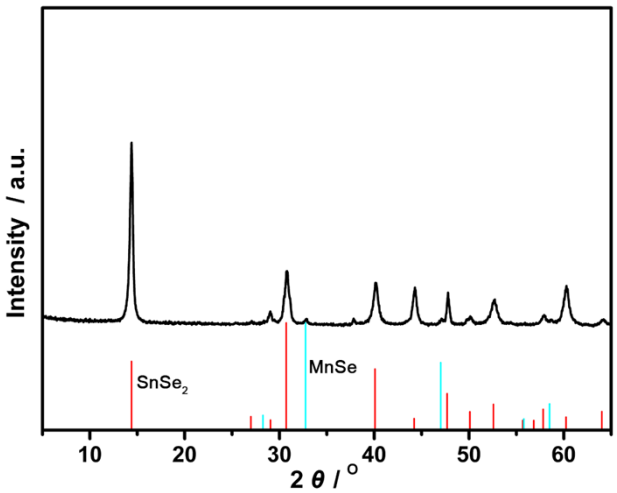

Figure S11. The PXRD pattern for the post-TGA residue of compound **4** along with the simulated ones of $SnSe_2$ and MnSe at bottom for comparison. The residue of compound **4** is identified as the mixture of $SnSe_2$ and MnSe.

3b). EDX spectra

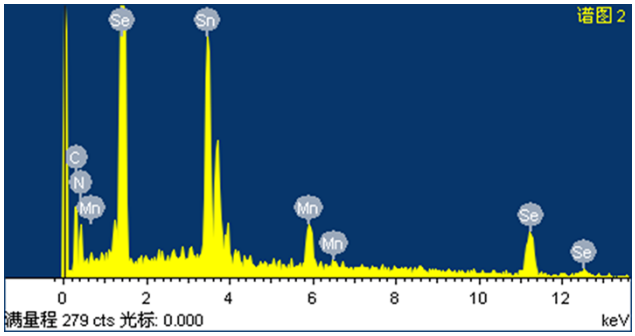

Figure S12. EDX spectrum of compound **1**.

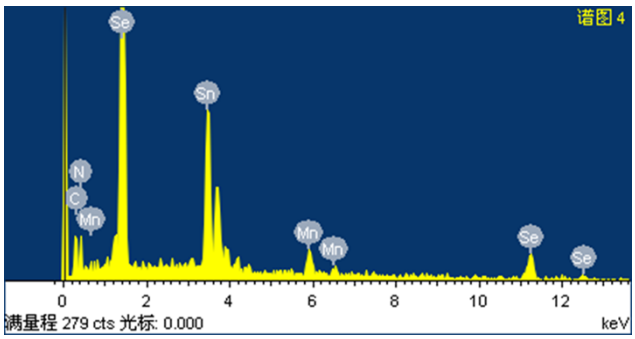

Figure S13. EDX spectrum of compound **2**.

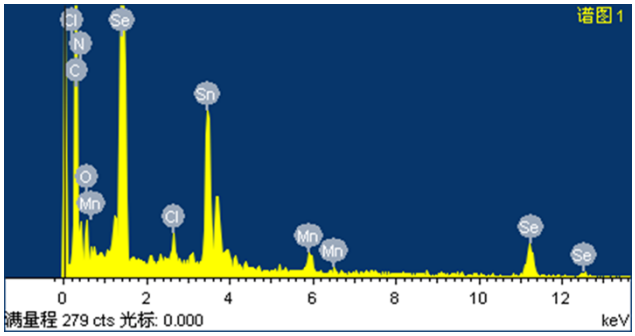

Figure S14. EDX spectrum of compound **3**.

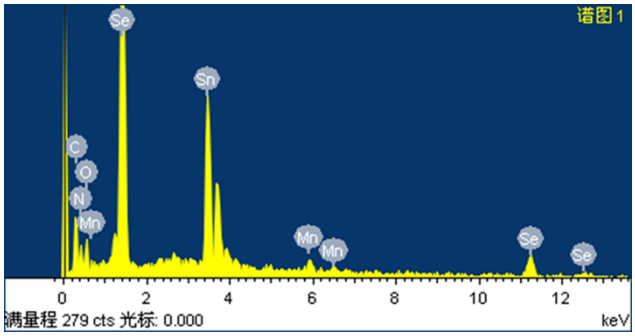

Figure S15. EDX spectrum of compound **4**.